Population Kinetics of a Repetitively-Pulsed Nanosecond Discharge

by

Benjamin T. Yee

A dissertation submitted in partial fulfillment
of the requirements for the degree of
Doctor of Philosophy
(Nuclear Engineering & Radiological Sciences)
in the University of Michigan
2013

Doctoral Committee:

Associate Professor John E. Foster, Chair
Doctor Edward V. Barnat, Sandia National Laboratories
Doctor Isaiah M. Blankson, National Aeronautics and Space Administration
Professor Augustus Evrard
Professor Mark J. Kushner

2013

I would like to dedicate this dissertation to someone else.

A C K N O W L E D G M E N T S

Who is this?

Preface

This is a dissertation about something; I really hope it's good.

TABLE OF CONTENTS

Dedication . . . . . **ii**

Acknowledgments . . . . . **iii**

Preface . . . . . **iv**

List of Figures . . . . . **vii**

List of Tables . . . . . **viii**

List of Appendices . . . . . **ix**

List of Abbreviations . . . . . **x**

Chapter

1 Introduction **1**

1.1 Overview 1
1.2 Literature Review 3
1.2.1 Early History of Pulsed Discharges 3
1.2.2 The Streamer Model 6
1.2.3 Ionizing Waves of Potential Gradient 7
1.2.4 RPNDS 9

2 Theory **12**

2.1 Plasmas 12
2.2 Atomic Spectroscopy 14
2.2.1 Spectral Lineshapes 16
2.2.2 Radiation Trapping 17

3 Experiment **18**

3.1 Discharge Apparatus 18
3.2 Measurement Conditions 19
3.3 Energy Coupling 20
3.4 Absorption Setup 20
3.4.1 Acquisition Process 21
3.5 Emissions Setup 22

4 Metastable Measurements **23**

5 Emission Measurements **24**

6 Modeling **25**

7 Conclusions **26**

Appendices **27**

Bibliography **29**

LIST OF FIGURES

1.1 A sketch of J.J. Thomson's early experiments on fast ionization waves in long vacuum tubes. 4

LIST OF TABLES

LIST OF APPENDICES

A Millimeter-Wave Interferometry **27**

B Rotational Spectroscopy **28**

LIST OF ABBREVIATIONS

RPND repetitively-pulsed nanosecond discharge

APP atmospheric-pressure plasma

VFP Vlasov-Fokker-Planck

EEDF electron energy distribution function

FIW fast ionization wave

CHAPTER 1

Introduction

1.1 Overview

Historically, the study of atmospheric-pressure plasmas (APP's) is indistinguishable from the study of plasmas as a whole. However, the detail of the measurements and calculations associated with APP's has been limited by their complexity. From a computational perspective, the high pressure and number of potential reactions present a difficult challenge. Likewise, the high pressure can significantly complicate the data analysis for a number of plasma diagnostics. Aside from the high pressures, the large electric fields, short time scales, and general randomness of APP's make even the most basic observations a feat.

In the last several decades, some of this has begun to change. High-powered computing has allowed simulations with remarkable detail. Similarly, advances in technology has enabled plasma diagnostics in regimes that were experimentally inaccessible. As a result, the body of knowledge regarding APP's has greatly increased. Sometimes, the motivation for this work is scientific curiosity. More often, the study of APP's has been driven by a broad range of applications.

Among the first plasma applications were provided by APP's: ozone generation and lighting. Aside from these items, plasma welding, polymer treatment, combustion, and plasma televisions have become widely accepted. Meanwhile, a large number of new applications may soon be added to this list, including: treatment of tissue wounds, altering airflow over

airfoils, and destruction of industrial pollutants.

Unsurprisingly, each case demands a different kind of plasma. The original arc discharges were created between two graphite rods connected to immense battery banks. In contrast, a modern research reactor studying plasma-assisted combustion might use a fast-switching semiconductor circuit. Over the years, several types of APPs have been developed for a variety of situations: dielectric-barrier, corona, thermal arc, RF, microwave, pulsed, and more.

Within this group[1], the repetitively-pulsed nanosecond discharge (RPND) has created considerable interest. Generally speaking, a RPND is a plasma generated by a repetitive electrical pulse applied between two electrodes. The pulse voltage is often in excess of one kilovolt, lasts anywhere from $< 1 - 100$ ns, and is repeated over a thousand times each second. The result is a wave of ionization (and light) which crosses from the powered electrode to the grounded one.

A RPND can fill volumes of several liters with a relatively uniform plasma. Though they can cause significant excitation of the background gas, they generally produce very little heating (in some cases below a detection limit of $\Delta \pm 15$ K). In addition, the excitation can be changed with adjustments to the magnitude or duration of the electrical pulse. Each of these characteristics are highly desirable in one or more of potential applications for APP's.

Given all of these promising properties, RPND's have been the subject of substantial study by several research groups. However, much of this work has focused on the physics of RPND's in air. Unfortunately, air's large number of constituent elements can lead to notable complexity. In turn, this can obscure some of the more fundamental questions relation to RPND's: how do they form, how is the energy distributed between excited particles, and what kind of spatial variation can be expected?

This paper details a study of each of these questions in a helium RPND. Specifically, the densities of one particular excited atom are measured for a variety of pressures and

[1]The interested reader is referred to Starikovskaia's review [1] which provides a general overview of APP's in the context of plasma-assisted combustion

locations. This is complemented by measurements of the light emissions for the same set of parameters. A simple model of a RPND is used to predict several characteristics of the plasma based on the excited state densities: electron density, electric field, and light emission. The measured light emissions are interpreted to show how the energy is distributed in the gas, and how it changes over time. Finally, they are compared with the estimated light emissions to check the validity of several common assumptions.

1.2 Literature Review

RPND's are only a recent invention which resulted from advances in fast-switching semiconductors. However, the physics of their formation is related to a much larger category of plasmas which includes lightning, sparks, and even some transient phenomena in DC glows. These plasmas are unique in that their formation occurs on timescales much faster than the traditional Townsend mechanism allows for. The means by which these plasmas form has acquired several names in the literature; here we will adopt the term, fast ionization wave (FIW).[2].

1.2.1 Early History of Pulsed Discharges

The first FIW was likely generated by Wheatstone in 1835 [2]. As reported by Thomson [3], Wheatstone built a vacuum tube six feet in length, and applied a high voltage across the gas. As a plasma formed in the tube, Wheatstone observed its formation with a rotating mirror. The use of this apparatus allowed Wheatstone to place a lower limit on the speed with which the plasma travelled from one electrode to the other. Though the discharge crossed the tube with a speed of at least 8×10^7 cm/s, spectral observations indicated that the particles emitting the light were not travelling at that speed [4].

[2]It should be noted that the phrase wave does not indicate any kind of periodic motion or spatial arrangement. Simply put, it describes a boundary which separates ionized and unionized gas which travels from one electrode to another.

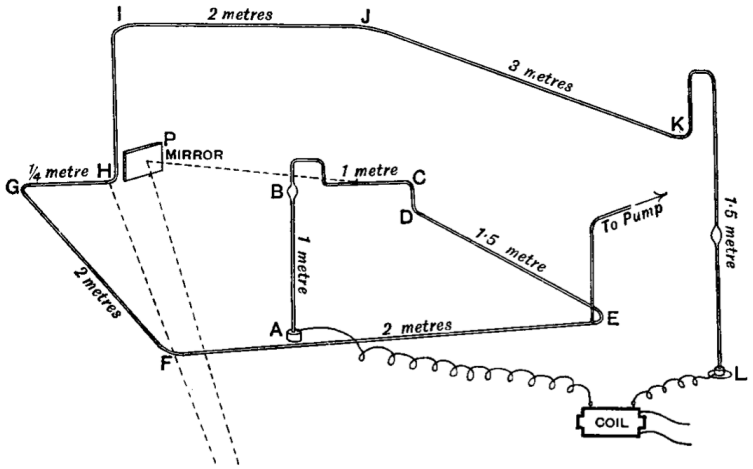

Figure 1.1: A sketch of J.J. Thomson's early experiments on fast ionization waves in long vacuum tubes.

Later, Thomson revisited this work with an improved apparatus [3]. This included a tube that was now 15 m in length and five mm in diameter, as seen in figure 1.1. Also using the rotating mirror apparatus, Thomson was able to greatly improve on the estimates of Wheatstone. He estimated that the so-called "luminous front" had a speed that was more than 1.5×10^{10}, or in excess of half of the speed of light. Furthermore, Thomson determined that the front always appeared to travel from the positively pulsed electrode (anode) to the ground electrode (cathode).

The study of these luminous fronts was revisited by several researchers in the wake of Thomson [5, 6, 7] with varied success. By his own admission, Beams's work in 1926 was done "hurriedly," using a rudimentary Kerr cell. In 1930, Beams returned to the propagation of light pulses in vacuum tubes with a rotating mirror apparatus [8]. In addition to confirming his previous measurements, and those of Thomson, Beams discovered that the FIW always traveled from the electrode with the highest absolute potential, to the lowest one. In other words, the wave could be anode or cathode directed, depending on the magnitude of their potentials relative to ground. Benefiting from an improved understanding of electricity, namely the existence of electrons and ions, Beams was able to provide the first hypothesis on the nature of the FIW:

> In the neighborhood of the electrode . . . the field is very high and intense ionization should take place. This ionization due to the large difference in mobilities of positive ions, negative ions and electrons respectively should result in the establishment of a space charge. This space charge, once formed near the high potential electrode Q must move down the tube regardless of the polarity of the applied potential because of the changes it produces in the field near its edges.

At about the same time, Schonland and Collens reported on their observations of lightning [9]. Though the general structure and length scale of lightning is substantially different from the luminous fronts observed by Beams and Thomson, the two phenomena would later prove to be very similar. In their work Schonland and Collens noted that lightning would usually occur in a two-step process. Based on the images they obtained, they suggested that the leader was generated by a relatively small "dart" with a mean vertical velocity of 7.2×10^8 cm/s. The dart moved in a random manner, changing directions at random intervals, but always moving downward.

The second step began when this dart reached the ground. Once there, a bright return stroke would occur along the same path that the leader had traced out. In contrast to the leader stroke, the return stroke had a velocity of 5×10^9 cm/s. Schonland and Collens hesitantly attributed the leader stroke to an extended electron avalanche, and the return stroke to thermal ionization along the conductive path generated by the dart. However, calculations by Cravath and Loeb showed that the speeds of the proposed avalanche would have to be inconsistent with the fields at the head of a lightning stroke [10]. Instead, they suggested that the dart was actually a moving region of space charge which locally accelerated electrons to ionizing energies. This was fundamentally similar to the mechanism proposed by Beams in 1930.

1.2.2 The Streamer Model

It was long known that sparks in air were similar to lightning. Advances in technology during the 1930's led to experiments which reinforced this similarity. In response to the measurements of Schonland and Collens; Snoddy, Beams, and Dietrich studied the breakdown of gas in a long tube with an oscillograph [11]. The results from the oscillograph showed a very clear return wave for which they measured several parameters the characterized as a function of pressure and applied potential. They observed that at low voltages, the system behaved like a large resistor in series with a capacitor, and below a critical voltage, no return stroke would form. Finally, in order to explain the propagation of the FIW generated by the positive pulse, they suggested that photoionization was occurring in the space ahead of the wave.

Around the same time, Flegler and Raether had come to a similar conclusion, leading to the first attempt at a theory describing streamers [12]. This same theory was proposed independently by Loeb and Meek in a series of papers [13, 14, 15]. The streamer theory divided the initial breakdown of a spark into two steps. In the first step, an electron avalanche is initiated between two electrodes. The avalanche travels toward the anode and leaves behind a region of high positive space charge. In the second step, the return stroke begins at the cathode and travels toward the cathode. It was suggested that the head of the return stroke ionizes the gas ahead of it by pulling in background electrons or via photoionization. [3].

The streamer model proved relatively successful in describing the development of sparks and lightning. Theoretical estimates of the speed matched the velocity measurements that were acquired through photographs and oscillographs. Additionally, the theory is able to account for the halting manner in which lightning is formed, though it is only tentatively

[3]These early works emphasized the importance of photoionization. It is now know that it is only required for cathode-directed streamers in systems with no background ionization. In addition, Mesyats later showed that the lifetime of the excited states responsible for photoionization were often longer than the lifetime of the streamers [16]

able to describe the branching and stepped appearance. Finally, the streamer mechanism provides an adequate explanation of why streamer discharges are not affected by the shape or material of the cathode, namely, they do not depend on secondary electron emission.

The study of the formation of streamers and lightning continues to be active to this day. Following the initial work of Flegler, Raether, Loeb, and Meek, a number of researchers began to explore the boundary between the Townsend mechanism and the streamer mechanism. Most notable was Fisher and Bederson's work in 1951 [17], which was later extended to nitrogen [18] and argon [**?**]. However, there were still a number of phenomena that were poorly explained by the streamer model. In particular, Kunhardt provided a useful overview of the problems in 1980 [19]. However, even before that, it was apparent that the transients of sparks and lightning was more complicated than thought.

1.2.3 Ionizing Waves of Potential Gradient

Per Chalmers [20], Rogowski and Buss [21, 22] observed a fast, diffuse, glow discharge immediately prior to the filaments which often accompany a streamer discharge. Allibone and Meek, noted similar diffuse discharges in air based on oscillographs and photographs [23, 24, 25]. However, the Boys apparatus which was employed in these studies (an ancestor to the modern streak camera) was unable to capture the evolution of the diffuse glow, given its large spatial extent.

This was first noted by Allibone who attempted to use Lichtenberg figures[4] to definitively capture this diffuse glow [26]. Later, Saxe and Meek used the recently invented photomultiplier tube to record the evolution of the light emissions in the brief, diffuse glow [27] as a function of space. Both studies agreed in the existence of the diffuse glow, despite some disagreement on the nature of its geometry and propagation.

The similarity of fast transient ionization waves in certain glow discharges [28] to those

[4]Such figures directly exposed photographic emulsions to the electrical discharge. The developed image was a time-integrated representation of the discharge.

observed in lightning and streamers led Loeb to to the conclusion that they were all the same phenomena [29]. He referred to them as "ionizing waves of potential gradient," as the proposed mechanism for the waves was the generation of a steep potential gradient in a sufficient short period of time.

As reported by Babich, Loika, and Tarasova [30], the detection of x-ray emissions from pulsed, high-pressure, helium discharges created a new avenue of interest for these transient plasmas [31, 32]. Unlike the streamers, which were often filamentary, these new discharges exhibited surprising uniformity. The primary difference being the duration of the pulse (on the order of nanoseconds) and the applied potentials (in excess of 200 kV).

The x-rays suggested that electrons in these discharges were accelerated to unusually high energies (on the order of 10 keV) despite the high collisionality. It was then that Babich and Stankevich suggested that the x-rays resulted from continually accelerated electrons impinging on the metal electrodes [33]. Briefly, the electric fields in the fronts of the ionizing waves were so large that they managed to accelerate electrons past the peak in their collisional cross sections.

Mesyats, Bychov, and Kremnev attempted to provide a more rigorous explanation for the uniform nature of these new discharges [16]. After conducting several experiments, they came to the conclusion that these transient plasmas were the result of many overlapping avalanches, unlike the streamer which only involves a single avalanche. Kunhardt and Byszewski later expanded on this work by developing a kinetic model to explain the behavior of all pulsed discharges above the Townsend threshold [19].

It was based on the studies of the fast electrons in these discharges that Mesyats, Bychov, and Kremnev proposed the use of a fast electron beam for pumping high-pressure gas lasers. Similar work was conducted simultaneously by Fenstermacher et al. [34]. Palmer [**?**], and Levatter and Lin [35] determined that there was a threshold amount of preionization required to ensure homogeneity of the discharge. Hunter [36], and Koval'chuk and Mesyats [37] later proposed that such discharges be used for fast-closing switches. Gas lasers and fast switches

would drive much of the later research on fast, pulsed discharges.

Eventually these discharges came to be referred to as fast ionization waves (FIWS). A large body of Russian literature developed around their study, though much of it has remained untranslated. In 1994, Vasilyak produced an extensive review of these studies [38]. The data include wave velocities for a variety of gases and pressures. Other parameters such as attenuation coefficients for the waves, high energy electron currents, electric field measurements, and a circuit model of the FIW are also included.

1.2.4 RPNDS

Beginning in 1998, the Moscow Institute of Physics and Technology (**mipt!**) produced a flurry of studies on the FIW [39, 40, 41]. They employed several different diagnostic techniques (photomultiplier tubes and capacitive probes) in an exceptionally detailed study in both air and nitrogen, using a shock tube and a bell jar. A summary of these investigations can be found in [42]. The work showed exceptionally reproducibility of the discharge parameters at relatively low repetition rates, on the order of tens of Hz, and evidence of runaway electrons. This work also included some of the first approximations of the electron energy distribution function (EEDF).

Interestingly, later analysis of a anode-directed FIW in nitrogen by the group at **mipt!** [43] concluded that the, the vast majority of the electrons were generated *after* the wave. This suggests that the ionization in an FIW does not strictly track the luminous front of the wave. Additionally, measurements of the conductivity suggested that the local approximation becomes invalid in the wave front and the electron energy distribution function resembles a beam.

In 1997 the invention of the fast ionization dynistor (**fid!**) was revealed [**?**]. These new devices enabled sub-nanosecond switching of 10's of kilovolts, with repetition rates approaching 100 kilohertz. This was a leap forward over previous technologies which generally used thyristors or spark gaps for switching. Particularly appealing was the high repeti-

tion rate of the **fid!**.

Recall that the volume-filling FIW required a significant amount of preionization. This was often accomplished an ionization source in addition to the high voltage pulse (in the form of UV radiation, or electron beams). However, the repetition rates of **fid!**s were high enough such that a substantial number of electrons would carry over between pulses. These seed electrons obviated the need for a preionization. In addition, the time-averaged densities of excited states could maintained at much higher values. This had particular promise for processing applications.

In the eventual commercialization of the **fid!** made economically feasible to create fast, repeatable fast ionization waves. It is this class of discharges which are now referred to as repetitively-pulsed nanosecond discharges, or RPNDS. Their uniformity, low gas heating, high-pressure operation, and efficient ionization made them attractive or a number of applications:

- plasma-assisted combustion [1],
- magneto-hydrodynamic energy bypass [44],
- plasma actuators [45],
- and high-pressure xenon lamps [46, 47].

Attention quickly turned toward plasma-assisted combustion [1], mhd energy bypass [44], and later, plasma actuators [45]. Additionaly studies, related to the development of high-pressure xenon lamps, led to several more quantitative models of the fiw development [46, 47]. These works also contributed to a semi-analytical energy coupling model as well [45].

Research efforts continued to use many of the same diagnostics as before. The current and voltage at the powered electrode were recorded (with varying levels of diligence), electric fields were measured with capacitive probes, and photomoultiplier tubes were used to

measure the progress of the luminous front. The 2000's did add a few new tools to the diagnostic arsenal. Perhaps the most common addition is the use of ICCD's in order to record transition and broadband light. This approach has been used to verify the reproducibility of the discharge [45]. Though the gate times are still too short to capture the development of the wave, excitation profiles like those initially demonstrated by Vasilyak[38] are commonly recorded. Another, more exotic addition, has been the use of CARS. This nonlinear technique has proven to be excellent at reproducing the spatial temperature profiles of pulsed nanosecond discharges. This has become particularly interesting for groups interested in applications to fast gas heating [48]. Others have used CARS to explore the electric field development of rpnds [49, 50]. Finally, another research group has used LCIF to detect the radial and axial profiles of the metastable and electron densities in a helium discharge. The CARS and LCIF approaches are both notable for being active diagnostics of direct properties. This allows unprecedented time resolution and detail.

CHAPTER 2

Theory

2.1 Plasmas

A volume containing some number of charged particles can be considered a plasma if it meets three conditions. The first requires that the motion of charged particles is primarily determined by the electric and magnetic fields of the volume rather than through collisions with neutral particles. This is classically expressed by the inequality

$$\sqrt{n_e e^2/(\varepsilon_0 m_e)} < \nu, \tag{2.1}$$

where n_e is the electron density, e is the fundamental charge, ε_0 is the permittivity of free space, m_e is the mass of an electron, and ν is the electron-neutral collision frequency. The left-hand side term is called the electron plasma frequency, it the characteristic frequency at which a plasma oscillates in response to a perturbation.

For a sufficiently large number of particles, the behavior of the each species of the plasma can be described by a continuous probability distribution function. This function, $f_\alpha(\vec{r}, \vec{v}, t)$, describes the probability of finding a particle of species α, at position $\vec{r}$, The distribution function for a particle can be determined by the Vlasov-Fokker-Planck VFP equation,

$$\frac{\partial f_\alpha}{\partial t} + \vec{v_\alpha} \cdot \nabla f_\alpha + q_\alpha \left(\vec{E} + \vec{v_\alpha} \times \vec{B}\right) \cdot \nabla_v f_\alpha = \left(\frac{\partial f_\alpha}{\partial t}\right)_{\text{coll}}. \tag{2.2}$$

Here, $\vec{E}$ is the electric field, $\vec{B}$ is the magnetic field, and $\partial f_\alpha/(\partial t)_{\text{coll}}$ is a term representing all collisions. The VFP equation is coupled to Maxwell's equations in order to obtain a self-consistent description of the particle distribution and the resulting fields. In essence, this is the Boltzmann equation from statistical mechanics, however it now includes several changes. Vlasov replaced the original force term with the Lorentz equation, and Fokker and Planck introduced the collision operator on the right-hand side. This is coupled with Maxwell's equations for a solution of the electric and magnetic fields in the plasma.

In the absence of external fields and with only elastic collisions, the equation admits the famous Maxwell-Boltzmann equilibrium distribution,

$$f_\alpha(v) = n\left(\frac{m_\alpha}{2\pi k_{\text{B}} T}\right)^{3/2} \exp\left(-\frac{m_\alpha v_\alpha^2}{2k_{\text{B}} T}\right), \tag{2.3}$$

where n is the number of degrees of freedom, k_{B} is Boltzmann's constant, and T is the temperature. A species of particles which possesses a Boltzmann distribution is said to be in equilibrium. Likewise, two species with the same distribution are in equilibrium.

Aside from this, the VFP equation is notoriously difficult to solve. As a result, most plasma models use various moments of equation 2.2 where the velocity dependence has been integrated out. These moments are the basis for the two-fluid equations, the MHD formulation, and global models. We will show the first three moments following the notation of Lieberman and Lichtenberg [51]. For example, the first moment is the continuity equation,

$$\frac{\partial n_\alpha}{\partial t} + \nabla \cdot (n_\alpha \vec{u_\alpha}) = G_\alpha - L_\alpha, \tag{2.4}$$

where $\vec{u_\alpha}$ is the mean velocity of species α, G_α is its rate of gain, and L_α is the rate of loss. This equation can be interpreted as the rate of change in particle density for a particular volume of space.

Though the continuity equation is much simpler than the original VFP equation, it cannot be solved alone. The mean velocity, $\vec{u}$, is undefined. Typically, this leads to the second

moment,

$$mn_\alpha \left[\frac{\partial \vec{u_\alpha}}{\partial t} (\vec{u_\alpha} \cdot \nabla) \right] = q_\alpha n_\alpha (\vec{E} + \vec{u_\alpha} \times \vec{B}) - \nabla \cdot \vec{\Pi_\alpha} + \vec{f}_{\alpha,\text{coll}} \tag{2.5}$$

where $\vec{\Pi_\alpha}$ is the pressure tensor, and $\vec{f}_{\alpha,c}$ is the rate of momentum transfer into species α. Again, any solution is stymied by the presence of a new a term, in this case, $\vec{\Pi_\alpha}$. At this point, an equation of state can be used to close the set of equations, in this case relating the pressure to the density. However, later work will benefit from one more moment.

Following the conservation of momentum, the energy conservation equation can be derived from the VFP equation,

$$\frac{\partial}{\partial t}\left(\frac{3}{2}p_\alpha\right) + \nabla \cdot \frac{3}{2}(p_\alpha \vec{u}_\alpha) + p_\alpha \nabla \cdot \vec{u}_\alpha + \nabla \cdot \vec{q}_\alpha = \frac{\partial}{\partial t}\left(\frac{3}{2}p_\alpha\right)\Big|_{\text{coll}} \tag{2.6}$$

where p_α is the species pressure, q_α is the heat flow vector, and the right-hand side is the time rate of change in energy as a result of collisions. In our case, we only consider the flux into the volume (from the electric field) and the distribution of this field via rate constants. This is the basis for the global model.

2.2 Atomic Spectroscopy

Spectroscopy spans a large body of theory which cannot be adequately covered here. Given that the measurements are all for helium, we will limit ourselves to a simple description of atomic spectroscopy. An atom is made of positively charged nucleus and a number of negatively charged electrons which orbit this nucleus. In the unperturbed, or ground state, the electrons occupy orbitals determined by a full solution of the Schrodinger equation.

However, interactions with other particles or photons can excite one or more of the electrons into orbitals with higher potential energy. In most cases relevant to low temperature plasmas, only a single electron will be excited at any given time. Depending on which orbital the electron is excited to, it can transition to orbitals with lower potential energy by

emitting a photon. These are typically called allowed transitions.

Each orbital in an atom can be described by four quantum numbers.

- n - The principal quantum number.
- l - Orbital angular momentum number.
- j - Total angular momentum.
- m_j - Total angular magnetic moment.

The Pauli exclusion principle restricts more than a single electron from occupying any given state defined by this series of numbers. Additionally, each set of numbers determines the potential energy possessed by an electron in that particular level.

Allowed transitions are determined by a series of selection rules. These selection rules can be summed up as the following:

- $\Delta S = 0$
- $\Delta L = \pm 1$

Though other transitions are possible (spin and dipole forbidden respectively), they tend to require an external perturbation in order to induce transition.

Figure shows the what is commonly called a Grotrian diagram for helium. In this diagram, the vertical axis represents the energy above the ground state, and the levels are arranged horizontally based on increasing L. Levels which are radiatively linked are connected by solid lines. As can be seen in this figure, only the levels having $S = 1$ are radiatively connected to the ground state. As a result, any helium atoms that are excited into the triplet manifold tend to stay there, accumulating in the metastable state, 2^3S.

Approaching 24 eV, the excited electron enters what is known as the continuum. The energy separation between states goes as n^{-2}, thus at large n the spacing becomes quite close and the states are almost indistinguishable. The levels are often referred to as Ryberg

states. Above 24.69 eV, the electron becomes totally detached from the helium nucleus, and all that remains is a singly ionized helium atom.

Though the emissions of ions can be quite useful in some plasmas, we do not concern ourselves with them in either the measurements or models. 24.69 eV is the largest known ionization potential, and as a result, the number of ions and the emissions associated with them remain relatively small.

2.2.1 Spectral Lineshapes

It is tempting to think that the energy spacing can be calculated exactly, however there is always some variance about a central energy. This is called the spectral lineshape, and it effects both the energy of the emitted photon in radiative transitions, and the photons that an atom can absorb. Though these variations can be attributed to quantum mechanical effects, the actual result can derived from the so-called dipole approximation.

In this case, we envision a single electron oscillating about a large, heavy, positive charge. The full details of this derivation are covered in Siegman [52], however we'll address some of the most pertinent portions here. The response of a collection of atoms to an applied electric field can be expressed as a quantity known as the susceptibility. This is generally defined as

$$\tilde{\chi}(\omega) \equiv \frac{\tilde{P}(\omega)}{\varepsilon_0 \tilde{E}(\omega)} \tag{2.7}$$

where $\tilde{\chi}$ is the electric susceptibility, $\tilde{P}$ is the macroscopic polarization, $\tilde{E}$ is the applied electric field, and ω is the frequency of the applied field.

Natural Linewidth The electric susceptibility often possesses both a real and imaginary component. Physically, these respectively represent the reactive and absorptive component of the medium. Accounting for level-dependent effects, the standard susceptibility for an

atomic transition can be written as

$$\tilde{\chi}_{\mathrm{at}}(\omega) = -j\frac{3}{4\pi^2}\frac{\Delta N\lambda^3\gamma_{\mathrm{rad}}}{\Delta\omega_{\mathrm{a}}}\frac{1}{1+2j(\omega-\omega_{\mathrm{a}})/\Delta\omega} \tag{2.8}$$

where ΔN represents the population difference between the upper and lower levels of the oscillator, λ is the transition wavelength, γ_{rad} is the natural radiative lifetime of the oscillator, $\Delta\omega_{\mathrm{a}}$ is the linewidth of the transition (for an unperturbed atom, this is simply γ_{rad}), and ω_{a} is the angular frequency of the transition or oscillator.

This equation is generally known as the complex lorentzian. Separated into its components it expresses both the absorptive and reactive properties of the atomic medium. It also clearly susceptible to fields that are displaced from ω_{a}. This is the finite linewidth associated with atomic emissions and absorption.

This linewidth affects each atom within the medium. Each atom will emit or absorb radiation with a probability described by this susceptibility. Consequently, this natural linewidth falls under the homogeneous category of line broadening.

Pressure Broadening Also included in this category is pressure broadening, or more fundamentally, dephasing.

2.2.2 Radiation Trapping

CHAPTER 3

Experiment

3.1 Discharge Apparatus

The discharge apparatus geometry was consistent with the design of a coaxial transmission line. This is similar to the design guidelines provided by Vasilyak [38]. The inner conductor is the plasma generated by the fast ionization wave. Surrounding that is a coaxial dielectric, in this case a quartz tube with 2.75" Conflat flanges on either side. Finally, surrounding the dielectric is the outer conductor or shield. In this case, the shield was an aluminum cylinder with slits of approximately 1.5" by 12" milled lengthwise. Figure **??** is a photograph of this discharge apparatus.

One flange of the quartz tube was held at ground potential, while the other flange was pulsed to approximately 7 kV. Given that the plasma undergoes significant decay between pulses, it is assumed that the impedance is almost infinite when the pulse is first applied, thus the actual voltage on the powered electrode is likely closer to 14 kV. The aluminum shield provides the ground connection for the ground electrode. The two were connected using a copper shim and a compressive shaft collar. The aluminum tube was connected to a second ground shield with a one inch copper braid. This second shield was made of copper and was separated by a teflon cylinder, with walls approximately 1" in thickness, from the powered electrode. Figure **??** is a schematic of the discharge apparatus.

Connected to the powered electrode was a Conflat nipple and an angled quartz window

used in the **lcif!** experiments. A short, silicone-coated, high voltage wire connected the window flange to the central conductor of an HN connector. The HN connector was seated on a square copper plate, which was pressed against the shield using four 10-32 screws.

The HN connector was used to attach the transmission line from the high voltage pulser. Initial experiments attempted to use N connectors, however these were susceptible to breakdown in the air gap which separated the center conductor from the outer shield. The transmission line was approximately 15 m in length. Observations, consistent with calculations, indicated that this provided a window of approximately 140 ns in which to make measurements before the reflected pulse returned to the system and re-energized the plasma.

Attached grounded flange was a second quartz envelope that isolated the ground electrode from the pumping section of the apparatus. Connected to the second quartz envelope was a stainless steel tee, one side of which was connected to an angled quartz window used for the **lcif!** experiments. The other side of the tee was isolated with an alumina break from a series of Conflat fittings connected to a roughing pump. The roughing pump was connected with a shutoff valve, as well as two bypass lines with inline needle valves for flow regulation.

3.2 Measurement Conditions

las!, emission, and coupling energy measurements were made at three different operating pressures. The operating pressures were: 0.3, 0.5, 1.0, 2.0, 3.0, 4.0, 8.0, and 16.0 Torr. Pressures below 10.0 Torr were measured with a capacitance manometer with a full scale range of 10.0 Torr, above this a capacitance manometer with a full scale range of 100.0 Torr was used.

Optical measurements were made at three locations along the axis of the discharge. The measurement location closest to the anode was separated from it by a distance of approximately six inches. Each other optical measurement location was moved further from the

anode by an additional three inches.

For each operating condition, measurements were made of the voltage and current. The voltage measurement was made via an internal divider from the power supply. Current measurements were made using an back-current shunt located at a break in the outer shield of the transmission line. The back-current shunt can be seen in Figure **??**. It is composed of nine, low impedance, one ohm resistors, connected in parallel. Each side of the resistors were soldered to a piece of copper foil which was then soldered to the outer shield. A calibrated DC power supply was used to measure the resistance of the current shunt.

All measurements were made using a LeCroy Waverider oscilloscope with a bandwidth of 1 GHz. Connections were made using minimal lengths of RG 50/U cable. When necessary for timing purposes, the cable lengths were matched. Connections were made using minimal lengths of RG 50/U cable. When necessary for timing purposes, the cable lengths were matched. All measurements which required maximum bandwidth were made with a using external 50 ohm terminators.

3.3 Energy Coupling

For comparison to other discharges, estimates of the energy coupling were made using the current and voltage characteristics at each operating pressure.

3.4 Absorption Setup

The **las!** setup was based upon the used of a distributed-feedback laser diode. Temperature and current control of the diode provided coarse and fine tuning, respectively, for the output frequency. It was found that it was unnecessary to adjust the temperature for the diode once the correct transition was found, therefore all tuning was accomplished using current tuning.

The laser diode was produced by Toptica Photonics (model #LD-1083-0070-DFB-1), and had a nominal operating power of 70 mW at a center wavelength of 1083 nm. The diode

was held inside a Toptica DL-100 diode housing which contained an integral thermoelectric cooler and collimating optics. The operation of the diode was controlled by a Toptica DC 110 monitor, DCC 110 current control, DTC 110 temperature control, and SC 110 scan control.

A schematic of the optical layout for the absorption experiment can be seen in Figure **??**. Immediately after exiting the housing, the beam was passed through an optical isolator in order to prevent instabilities from back reflections. Next the beam was attenuated using a neutral density filter in order to keep its intensity below the saturation level for the transition. Following that, the beam passed through two apertures for alignment. Here, the beam was split by a partially reflecting mirror. Approximately 98% of the beam was allowed to pass through to a reference photodiode (Thorlabs DET300). After passing through the plasma, entered another aperture to limit near-coincident plasma emissions. The background emissions were further reduced using a long pass filter with a cutoff of 1000 nm. Finally, the beam was coupled into an optical fiber which connected to the detection electronics.

The transmitted laser light was detected with an InGaAs photodiode (Thorlabs DET410). The signal from the diode was often too small to detect, so the output of the signal photodiode was sent through a voltage amplifier (Femto HVA-200M-40-B). The light response of this system is limited by the photodiode which has a nominal rise time of five nanoseconds. The signal from the amplifier was terminated by a 50 ohm terminator and sensed by the aforementioned oscilloscope.

3.4.1 Acquisition Process

The actual acquisition process required a specific series of steps in order to properly account for all noise sources. In order to accommodate this process, a custom LabView script was used to automate the acquisition of the laser transmission spectra. Generally speaking, the

signal can be described as

$$V_{\text{total}} = V_{\text{signal}} + V_{\text{background}} + V_{\text{plasma}}. \tag{3.1}$$

In order to remove the background signal, the acquisition scr

3.5 Emissions Setup

CHAPTER 4

Metastable Measurements

CHAPTER 5

Emission Measurements

CHAPTER 6

Modeling

CHAPTER 7

Conclusions

APPENDIX A

Millimeter-Wave Interferometry

$$e = mc^2 \tag{A.1}$$

APPENDIX B

Rotational Spectroscopy

BIBLIOGRAPHY

[1] S M Starikovskaia. Plasma assisted ignition and combustion. *Journal of Physics D: Applied Physics*, 39(16):R265–R299, August 2006.

[2] C. Wheatstone. Versuche, die Geschwindigkeit der Elektricität und die Dauer des elektrischen Lichts zu messen. *Annalen der Physik und Chemie*, 110(3):464–480, 1835.

[3] J J Thomson. *Notes on Recent Researches in Electricity and Magnetism*. Clarendon Press, Oxford, UK, 1893.

[4] W. v. Zahn. Spectralröhren mit longitudinaler Durchsicht. *Annalen der Physik und Chemie*, 244(12):675–675, 1879.

[5] John James. Die Abraham-Lemoinesche Methode zur Messung sehr kleiner Zeitintervalle und ihre Anwendung zur Bestimmung der Richtung und Geschwindigkeit der Entladung in Entladungsröhren. *Annalen der Physik*, 320(15):954–987, 1904.

[6] R. Whiddington. The Discharge of Electricity through Vacuum Tubes. *Nature*, 116(2918):506–509, October 1925.

[7] J. Beams. The Time Interval Between the Appearance of Spectrum Lines in Spark and in Condensed Discharges. *Physical Review*, 28(3):475–480, September 1926.

[8] J. Beams. The Propagation of Luminosity in Discharge Tubes. *Physical Review*, 36(5):997–1001, September 1930.

[9] B. F. J. Schonland and H. Collens. Development of the Lightning Discharge. *Nature*, 132(3332):407–408, September 1933.

[10] a. M. Cravath and L. B. Loeb. The Mechanism of the High Velocity of Propagation of Lightning Discharges. *Physics*, 6(4):125, 1935.

[11] L. Snoddy, J. Beams, and J. Dietrich. The Propagation of Potential in Discharge Tubes. *Physical Review*, 50(5):469–471, September 1936.

[12] E. Flegler and H. Raether. Der elektrische Durchschlag in Gasen nach Untersuchungen mit der Nebelkammer. *Zeitschrift f r Physik*, 99(9-10):635–642, September 1936.

[13] Leonard B. Loeb and John M. Meek. The Mechanism of Spark Discharge in Air at Atmospheric Pressure. I. *Journal of Applied Physics*, 11(6):438, June 1940.

[14] Leonard B. Loeb and J. M. Meek. The Mechanism of Spark Discharge in Air at Atmospheric Pressure. II. *Journal of Applied Physics*, 11(7):459, 1940.

[15] J. Meek. A Theory of Spark Discharge. *Physical Review*, 57(8):722–728, April 1940.

[16] Gennadii A Mesyats, Yu I Bychkov, and V V Kremnev. Pulsed nanosecond electric discharges in gases. *Soviet Physics Uspekhi*, 15(3):282–297, March 1972.

[17] L. Fisher and B. Bedderson. Formative Time Lags of Spark Breakdown in Air in Uniform Fields at Low Overvoltages. *Physical Review*, 81(1):109–114, January 1951.

[18] G. Kachickas and L. Fisher. Formative Time Lags of Uniform Field Breakdown in N2. *Physical Review*, 88(4):878–883, November 1952.

[19] E Kunhardt and W Byszewski. Development of overvoltage breakdown at high gas pressure. *Physical Review A*, 21(6):2069–2077, June 1980.

[20] I D Chalmers. The transient glow discharge in nitrogen and dry air. *Journal of Physics D: Applied Physics*, 4(8):1147–1151, August 1971.

[21] W Rogowski, E. Flegler, and R. Tamm. Über Wanderwelle und Durchschlag. *Archiv für Elektrotechnik*, 18(5):479–512, September 1927.

[22] K. Buss. Der Stufendurchschlag. *Archiv für Elektrotechnik*, 26(4):266–272, April 1932.

[23] T E Allibone and J M Meek. The Development of the Spark Discharge. II. *Proceedings of the Royal Society A: Mathematical, Physical and Engineering Sciences*, 169(937):246–268, December 1938.

[24] T. E. Allibone and J. M. Meek. The Development of the Spark Discharge. *Proceedings of the Royal Society A: Mathematical, Physical and Engineering Sciences*, 166(924):97–126, May 1938.

[25] T E Allibone. The Mechanism of a Long Spark. *Journal of the Institute of Electrical Engineers*, 82(497):513–521, 1938.

[26] T E Allibone. Development of the Spark Discharge. *Nature*, 161(4103):970–971, June 1948.

[27] R F Saxe and J M Meek. Development of Spark Discharges. *Nature*, 162(4111):263–264, August 1948.

[28] Russell Westberg. Nature and Role of Ionizing Potential Space Waves in Glow-to-Arc Transitions. *Physical Review*, 114(1):1–17, April 1959.

[29] L B Loeb. Ionizing Waves of Potential Gradient: Luminous pulses in electrical breakdown, with velocities a third that of light, have a common basis. *Science (New York, N.Y.)*, 148(3676):1417–26, June 1965.

[30] L P Babich, T. V. Loiko, and L. V. Tarasova. The physics of high-voltage nanosecond discharges in dense gases. *Radiophysics and Quantum Electronics*, 20(4):436–442, April 1977.

[31] Yu L Stankevich and V G Kalinin. Fast electrons and X-radiation in the initial stage of pulse spark discharge development in air. *Doklady Akademii Nauk*, 177:72–73, 1967.

[32] R. C. Noggle. A Search for X Rays from Helium and Air Discharges at Atmospheric Pressure. *Journal of Applied Physics*, 39(10):4746, 1968.

[33] L P Babich and Yu L Stankevich. Transitions from streamers to continuous electron acceleration. *Soviet Physics Technical Physics*, 17:1333, 1973.

[34] C. a. Fenstermacher. Electron-Beam-Controlled Electrical Discharge as a Method of Pumping Large Volumes of CO2 Laser Media at High Pressure. *Applied Physics Letters*, 20(2):56, 1972.

[35] Jeffrey I. Levatter and Shao-Chi Lin. Necessary conditions for the homogeneous formation of pulsed avalanche discharges at high gas pressures. *Journal of Applied Physics*, 51(1):210, 1980.

[36] R O Hunter. Electron beam controlled switching. In *International Pulsed Power Conference*, pages IC8–1 –IC8–6, New York, NY, 1976. Institute of Electrical Engineers, Inc.

[37] B M Koval'chuk and G A Mesyats. Rapid cutoff of a high current in an electron-beam-excited discharge. *Soviet Technical Physics Letters*, 2(252), 1976.

[38] L M Vasilyak, S V Kostyuchenko, N N Kudryavtsev, and I V Filyugin. Fast ionisation waves under electrical breakdown conditions. *Physics-Uspekhi*, 37(3):247–268, March 1994.

[39] N B Anikin, S V Pancheshnyi, S M Starikovskaia, and A Yu Starikovskii. Breakdown development at high overvoltage: electric field, electronic level excitation and electron density. *Journal of Physics D: Applied Physics*, 31(7):826–833, April 1998.

[40] S.V. Pancheshnyi, S.M. Starikovskaia, and A.Yu. Starikovskii. Measurements of rate constants of the v =0) and v =0) deactivation by N2, O2, H2, CO and H2O molecules in afterglow of the nanosecond discharge. *Chemical Physics Letters*, 294(6):523–527, September 1998.

[41] S M Starikovskaia, a Yu Starikovskii, and D V Zatsepin. The development of a spatially uniform fast ionization wave in a large discharge volume. *Journal of Physics D: Applied Physics*, 31(9):1118–1125, May 1998.

[42] S M Starikovskaia, N B Anikin, S V Pancheshnyi, D V Zatsepin, and A Yu Starikovskii. Pulsed breakdown at high overvoltage: development, propagation and energy branching. *Plasma Sources Science and Technology*, 10(2):344–355, May 2001.

[43] S V Pancheshnyi, S M Starikovskaia, and A Yu Starikovskii. Population of nitrogen molecule electron states and structure of the fast ionization wave. *Journal of Physics D: Applied Physics*, 32(17):2219–2227, September 1999.

[44] S.O. Macheret, M.N. Shneider, and R.B. Miles. Modeling of air plasma generation by repetitive high-voltage nanosecond pulses. *IEEE Transactions on Plasma Science*, 30(3):1301–1314, June 2002.

[45] Igor V Adamovich, Munetake Nishihara, Inchul Choi, Mruthunjaya Uddi, and Walter R Lempert. Energy coupling to the plasma in repetitive nanosecond pulse discharges. *Physics of Plasmas*, 16(11):113505, 2009.

[46] Dmitry S. Nikandrov, Lev D. Tsendin, Vladimir I. Kolobov, and Robert R. Arslanbekov. Theory of Pulsed Breakdown of Dense Gases and Optimization of the Voltage Waveform. *IEEE Transactions on Plasma Science*, 36(1):131–139, 2008.

[47] L D Tsendin and D S Nikandrov. An analytical approach to planar ionization fronts in dense gases. *Plasma Sources Science and Technology*, 18(3):035007, August 2009.

[48] Yvette Zuzeek, Inchul Choi, Mruthunjaya Uddi, Igor V Adamovich, and Walter R Lempert. Pure rotational CARS thermometry studies of low-temperature oxidation kinetics in air and ethene–air nanosecond pulse discharge plasmas. *Journal of Physics D: Applied Physics*, 43(12):124001, March 2010.

[49] Osaka University) Ito, Tsuyohito (Frontier Research Base For Global Young Researchers, Osaka University) Kobayashi, Kazunobu (Center For Atomic And Molecular Technologies, Ruhr-University Bochum) Czarnetzki, Uwe (Institute For Plasma And Atomic Physics, and Osaka University) Hamaguchi, Satoshi (Center For Atomic And Molecular Technologies. Rapid formation of electric field profiles in repetitively pulsed high-voltage high-pressure nanosecond discharges. *Journal of Physics D: Applied Physics*, 43(6):062001, February 2010.

[50] Tsuyohito Ito, Kazunobu Kobayashi, Sarah Müller, Uwe Czarnetzki, and Satoshi Hamaguchi. Electric field measurements at near-atmospheric pressure by coherent Raman scattering of laser beams. *Journal of Physics: Conference Series*, 227:012018, May 2010.

[51] Michael A. Lieberman and Allan J. Lichtenberg. *Principles of Plasma Discharges and Materials Processing*. John Wiley & Sons, Inc., Hoboken, NJ, USA, 2nd edition, April 2005.

[52] A. E. Siegman. *Lasers*. University Science Books, Sausalito, CA, 1986.